Iranian Journal of Materials Science and Engineering, Vol. 20, Number 3, September 2023
REASERCH PAPER

Hardness and Wear Characteristics of Laser-Clad WC-17Co Coatings on AISI H13 and AISI 4140 Steel

Fábio Edson Mariani[1], Gabriel Viana Figueiredo[1], Germán Alberto Barragán de Los Rios[2,*], Luiz Carlos Casteletti[1], Reginaldo Teixeira Coelho[1]

* *german.barragan@upb.edu.co*

[1] University of São Paulo/São Carlos School of Engineering, 400 Trabalhador São Carlense Ave., Sao Carlos, 13140-170, Sao Paulo, Brazil
[2] Grupo de investigación en Ingeniería Aeroespacial, Universidad Pontificia Bolivariana, Circular 1 # 70-01, Medellín, Colombia

Received: March 2023 **Revised: September 2023** **Accepted: September 2023**
DOI: 10.22068/ijmse.3206

Abstract: *Elevating component performance through advanced surface coatings finds its epitome in the domain of laser cladding technology. This technique facilitates the precision deposition of metallic, ceramic, or cermet coatings, accentuating their superiority over conventional methods. The application spectrum for laser-clad metallic coatings is extensive, encompassing critical components. Central to the efficacy of laser cladding is the modulation of laser parameters—encompassing power, speed, and gas flow—which decisively influence both process efficiency and coating properties. The meticulous calibration of these parameters holds the key to producing components endowed with refined attributes while ensuring the sustainable continuation of the process. As such, this study embarks on an empirical investigation aimed at transcending existing process limitations. It delves into the characterization of laser-clad WC-17Co coatings on AISI H13 and AISI 4140 steels. The importance of WC-17Co coatings lies in their capacity to enhance wear resistance, extend component life, reduce maintenance costs, and improve the performance of various industrial components across diverse sectors. On the other hand, the substrates have pivotal roles. AISI H13 is lauded for its exceptional hot work capabilities, while AISI 4140 steel is renowned for its robust strength and endurance. Through rigorous evaluation, the resultant deposited coatings offer crucial insights into the efficacy of manufacturing parameters. Employing a comprehensive suite of analytical techniques including laser confocal microscopy, Vickers microhardness assessment, and micro-adhesive wear testing, the study thoroughly characterizes the samples. The outcomes underscore the achievement of homogenous coatings marked by elevated hardness and exceptional wear resistance, thereby signifying a substantial enhancement over the substrate materials.*

Keywords: *Laser cladding, AISI H13, AISI 4140, WC-17Co, Coatings, Micro-adhesive wear tests.*

1. INTRODUCTION

The improvement of industrial parts and tools through the advancement of technology has led to significant progress in engineering in terms of innovation, economic, and environmental efficiency. A promising approach to improve the surface properties of industrial components is the application of layers or coatings with proper-ties superior to those of the substrate. Many researchers produced coatings utilizing various techniques, such as spraying (high-velocity oxygen-fuel HVOF, thermal and plasma spray) [1–3]; thermochemical treatments (nitriding) [4]; deposition [5–7]; and laser cladding [8]. Understanding the interconnections between these technologies, process parameters, and quality is an essential step in the development of coatings and has been extensively studied [9–18]. Laser cladding employs a high-energy beam to add coating material to the substrate surface forming a clad-ding layer that is metallurgical bonding by fusion [19, 20]. So, the technology involves numerous parameters and interactions that increase the process's complexity [21]. Nevertheless, the process allows for obtaining unique, duplex, or multiplex coatings that conventional processes cannot produce. Moreover, diverse materials can be employed during the process, which enables the production of coatings with different properties along their thickness, increasing the toughness and surface charge capacity, together with a more outstanding adhe-sion between layers [22].

The coatings obtained by laser cladding can be tailored to meet specific application requirements through careful selection of coating materials, process parameters, and post-processing treatments. Among the char-acteristics to be highlighted in the coatings obtained by this

[DOI: 10.22068/ijmse.3206]

method, we find, high hardness, strong corrosion resistance, wear resistance, oxidation resistance, low porosity, large thicknesses [23], and excellent metallur-gical adhesion with the substrate when compared with other coatings procedures [24–26]. Nevertheless, the coating shows defects and residual tensions in some cases due to the fast heating and cooling. Therefore, many studies have attempted to enhance the coating quality by altering the process parameters to address the issues caused by the technique.

One of the most promising materials for coatings is the raw materials based on WC-Co. Its excellent wear resistance behavior follows the combination of high hardness and toughness from carbide and Co binding ma-trix. As a result, WC-Co cermet materials are frequently utilized as protective coatings of wear-resistant com-ponents in various areas (e.g., aerospace, automobile, petrochemical, and equipment manufacturing) [10].

Research carried out with WC-Co deposition by thermal spray HVOF demonstrated that using this composi-tion as a coating provides good resistance to adhesive and abrasion wear [10, 27], as well as high hardness and good tenacity. However, WC-Co coatings produced by thermal spraying are prone to the presence of some porosity, surface roughness, and decarburization. As a result, WC proportion decreases upon forming W, W2C, and amorphous or monocrystalline Co-W-C phases, such as Co3W3C and CO6W6C-η-phases. These phases have lower hardness and low tenacity compared to WC-Co, which can reduce the wear resistance of the coating [23, 28].

Using a laser energy source to produce WC-Co coatings can provide promising results compared to thermal spraying or HVOF regarding heat-affected zone, hardness, and wear behavior. However, laser deposition can also lead to the dissolution and precipitation of other fragile phases depending on laser power, particle size, and volume fractions. Therefore, the process parameters must be carefully controlled so that carbide dissolu-tion does not occur [10, 29–32].

Limited works in the literature have been undertaken concerning WC-Co coatings fabricated through the la-ser cladding powder-fed process. Therefore, the intricate interplay between process parameters and resultant coating attributes has been subject to comprehensive investigation across diverse substrate-coating consolida-tions [33, 34]. Consequently, this research endeavors to assess and ascertain the adequate deposition param-eters within the laser cladding methodology for the synthesis of WC-17Co coatings onto AISI H13 and AISI 4140 steel substrates. The assessment of WC-17Co coating integrity was pursued by using an analysis en-compassing the tribological attributes of the deposited coating. Specifically, in terms of microhardness and wear characteristics, they are commonly used tests to evaluate coatings [35, 36]. The strategic harmonization of cladding materials and substrates ensures the tailored production of coatings that align precisely with speci-fied performance prerequisites, thus culminating in the augmentation of the overall tribological profile of the substrate. This, in turn, imparts substantive advantages to an extensive array of industrial and commercial domains.

2. EXPERIMENTAL PROCEDURES

2.1. Materials

Two distinct substrate sheets composed of steel were chosen as specimens for the experimental investiga-tion. One substrate entails AISI H13 steel, renowned for its prevalent utilization in the fabrication of hot work tooling encompassing applications such as die casting, extrusion, and forging dies. The other substrate, AISI 4140 steel, is notably employed in diverse roles including the production of gears, shafts, and axles. These substrates, each possessing a uniform thickness of 5 mm, were judiciously selected to serve as the founda-tional basis of the experiment.

The rationale underpinning the selection of these specific substrate materials emanates from their indispen-sably coveted attributes of wear resistance, which correspond harmoniously to the exigencies of their desig-nated operational domains. By employing these substrates, the inquiry extends to the assessment of the viabil-ity of the coating material technique across distinct operational contexts, notwithstanding the inherent diver-gence in their chemical compositions and mechanical traits. This approach offers a comprehensive framework for evaluating the applicability and adaptability of the coating technique across disparate industrial settings.

The specimens were meticulously subjected to a

[DOI: 10.22068/ijmse.3206]

series of treatments as outlined in Table 1. Notably, an austempering process was meticulously administered across two discrete temperature thresholds. The deter-mination of these austempering temperatures engendered a judicious amalgamation of pertinent material char-acteristics, desired outcomes, comprehensive literature appraisal, and antecedent research undertakings.

Subsequently, the specimens were subjected to meticulously orchestrated isothermal quenching procedures employing oil-based mediums. This strategic approach aimed at eliciting a specific microstructural configura-tion that not only engenders the coveted mechanical attributes but also confers augmented resistance to wear phenomena.

An inherent virtue of the austempering process resides in its characteristic proclivity for gradual cooling rates. This deliberate moderation in cooling kinetics serves to abate the proclivity towards distortion and fracture, both of which constitute substantial concerns. This attribute, in turn, bestows upon the speci-mens a heightened performance profile during operational deployment.

For the cladding material, a commercially available conventional WC-17Co powder is characterized by par-ticles spanning a size spectrum of 15 to 45 μm. The structural attributes of the powder were subjected to scru-tiny through the application of a confocal microscope, yielding insights visualized in Figure 1, alongside the concomitant outcomes of the particle size distribution analysis.

The determination of the cladding material was predicated upon exhaustive bibliographic assessments, wherein this specific cermet material found application owing to its remarkable and multifaceted attributes. These attributes, collectively encompassing an array of exceptional properties, render it amenable for deploy-ment as a protective coating on components necessitating resistance to wear within diverse domains by the selected substrates.

2.2. Methods

The coating material deposition was conducted in a preplaced powder configuration (see Figure 2), employ-ing the BeAM® Modulo 250 machine, a five-continuous axis Laser-Based Direct Energy Deposition (DED-LB) system. It is equipped with a coaxial nozzle and a 1000 W Nd-YAG laser and is controlled by the Siemens® 840D unit [37].

Table 1. Heat treatment conditions

Material	Austenitization		Tempering	Quenching	
	Temperature	Time		Temperature	Time
AISI H13	1030°C	4 hours	Oil	540°C	2 hours
AISI4140	870°C	4 hours	Oil	200°C	1 hour

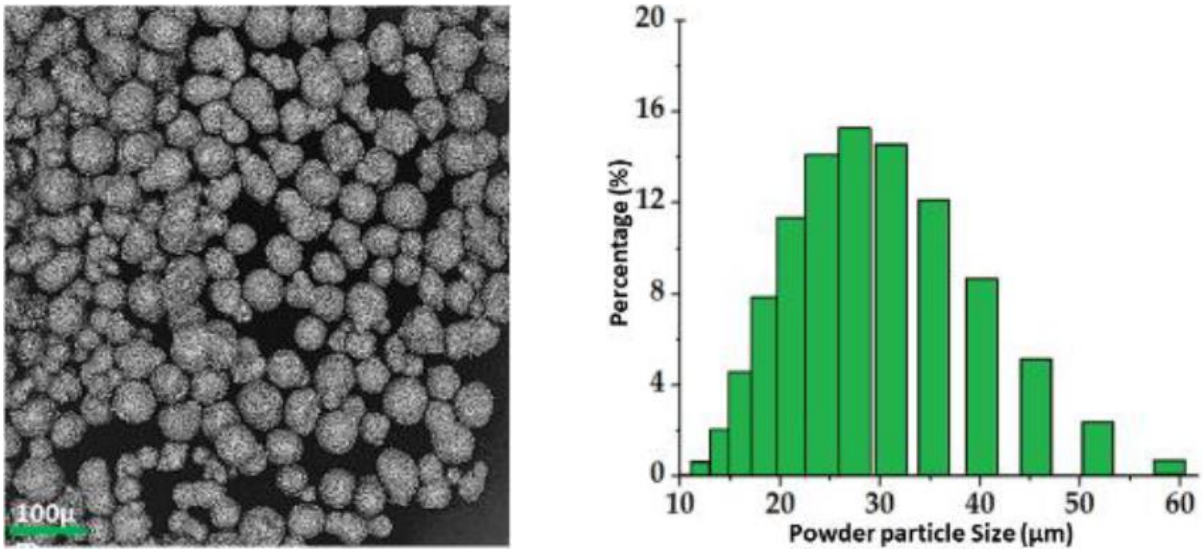

(a) (b)

Fig. 1. WC-17Co powder a) confocal image and b) powder particle size distribution.

[DOI: 10.22068/ijmse.3206]

The deposition head was located 3.5 mm over the substrate for the deposition process. Different parameters were used to produce linear strokes of 15 mm separated from each other later to evaluate the result of the variation of each parameter. Two deposition speeds (300 and 500 mm/min) and three laser powers (250, 350, and 450 W) were used, allowing six different configurations for the study. During the coating process, Argon was used to protect the laser and weld pool from contamination or oxidation, being applied coaxially by the deposition head from 3 flows: nozzle (3l/min), carrier (3l/min), and former (6l/min). These parameters were selected considering the results of previous experiments for manufacturing coatings over steel plates using the same equipment presented in [38], in which good protection characteristics of the fusion zone and optical equipment were obtained.

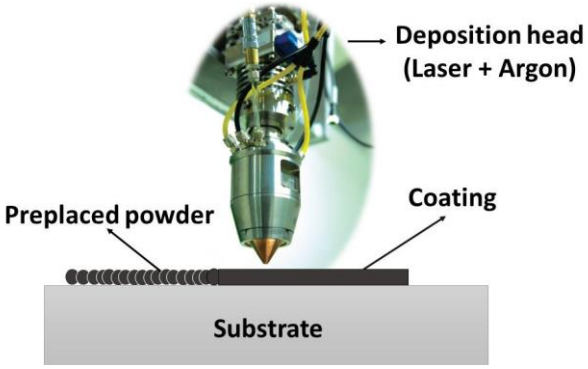

Fig. 2. Schematic of preplaced powder cladding process.

After the cladding process, deposition lines were analyzed in terms of geometry, porosity, adhesion, and Heat Affected Zone (HAZ) extension. The process parameters combination that offered the best results was selected to conduct a coating on a study area for specific test developments. The overlapping, defined as the percentage in which one trace overlaps the other to produce surfaces free of pores and uniformly avoiding roughness on the final surface was defined as 1/3 of the line width.

2.3. Metallographic Observation

The samples were identified and embedded for metallographic observation to detect the cross-sectional re-gion. Then, they were sanded and polished (using SiC sandpaper: 80, 140, 220, 320, 400, 600, 1000, and 1200 mesh) and 0.05 µm alumina solution. For the microstructural visualization of AISI 4140 steel, a chemical attack was carried out with Nital 2% (2 ml HNO_3 + 98 ml ethyl alcohol) for 10 seconds, for AISI H13 steel, the chemical reagent Vilella (5 ml HCl + 2 g picric acid + 100 ml ethyl alcohol) for 10 seconds. After metallographic preparation, coatings were analyzed using laser confocal microscopy, using equipment manufactured by Olympus®, model OLS4000, with an integrated camera.

2.4. Microhardness Tests

To analyze the hardness of the produced substrates and coatings, Vickers microhardness (HV) tests were performed, using a Buheler® microdurometer, model 1600-6300, following the ASTM E384-17 standard [39], with a load time of 15 seconds and a load of 200 gf. In addition to the average hardness, measurements of the coating hardness were also obtained according to the distance from the surface (microhardness profiles), mak-ing a series of measurements with a pre-defined spacing between them to assess the evolution of this surface property towards the center of the sample.

2.5. Wear Tests

The wear assessments encompassed an evaluation of the wear resistance exhibited by both the coatings gen-erated and the underlying substrates. Figure 3, presents a schematic of the employed test machine. The test was carried out on samples after sanding using sandpaper of 80, 140, 220, 320, 400, 600, 800, 1000, and 1200 mesh; and polished in 0.05 µm alumina suspension. The goal of the preparation process is to obtain a smooth area, free from any interference, for a micro-scale test. For each test, a 1-inch ball of AISI 52100 steal was utilized. The ball was cleaned correctly to avoid nosiness. Four tests were carried out with different dura-tion times, 5, 10, 15, and 20 minutes, with a load of 300 g = 5.25 N, under the same speed of 265 rpm. More information about the test can be found in [40–43].

Each test was repeated four times in each sample to obtain the volumes removed means and respective standard deviations. These parameters were defined to prevent any interfacial element from influencing the effect of microstructural characteristics during the tests. First, the products of these tests were

[DOI: 10.22068/ijmse.3206]

weathered re-gions in the form of a cap, with their average diameters used to obtain worn volumes. Then, the distances traveled, and the average volumes removed were obtained from the average diameters of the caps resulting from the friction between the sphere and the sample. No significant wear debris was produced during the test-ing.

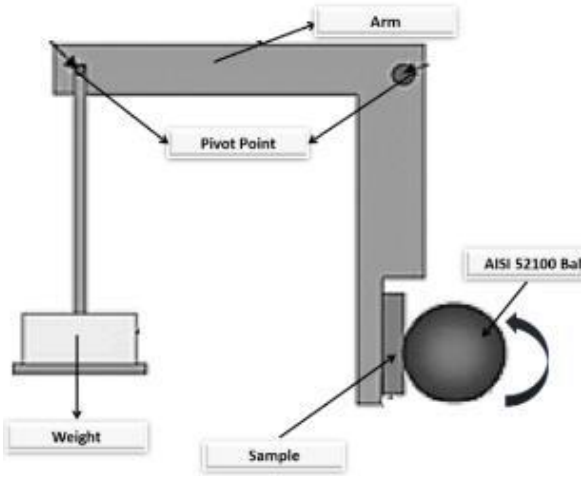

Fig. 3. Test machine schematic.

3. RESULTS

The following figures show the optical micrographs of the transverse sections of the deposited layers and their corresponding parameter values of laser power and travel speed employed. The first depositions aimed to verify the best parameters for the composition selected for the study, WC-17Co, as cladding material over AISI 4140 and AISI H13 steel substrates. Figures 4 and 5 show the results obtained for AISI 4140 substrate.

The results of the cladding process with the travel speed setup in 300 mm/min are the following. A non-deposition condition when the lowest laser power of 250 W is employed (a), a very irregular deposition for 350 W of power (b), and a porous coating for the case in which the greater power (450 W) was employed (c). For all the cases of travel speed defined in 500 mm/min, WC-17Co coating was presented. However, in condition (c), laser power 450 W, despite having resulted in a reasonable amount of deposited material, was not attrac-tive due to the large HAZ region. In Figure 5 the results of cladding applied when the velocity was set at 500 mm/min and the laser power in 250W (a), 350 W (b) and 450W (c) can be observed.

In figure 6 AISI H13 substrate is employed to conduct the depositions. In all the images the velocity was defined in 300 mm/min and different sets of laser power were employed (a) 250 W, (b) 350 W, and (c) 450 W.

In Figure 7 the depositions conducted over AISI H13 substrate employing a 500 mm/min velocity and dif-ferent laser power settings (a) 250 W, (b) 350 W, and (c) 450 W are presented.

For all the cases presented in Figure 6 and 7 is possible to observe that the behavior of the coatings is simi-lar to that presented with the AISI 4140 substrate.

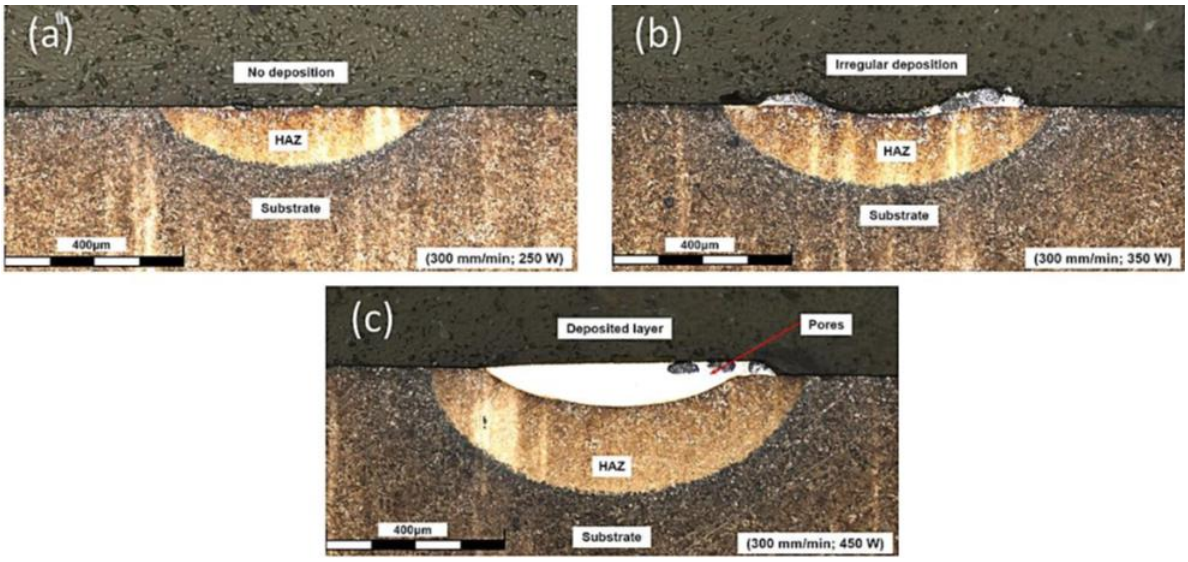

Fig. 4. Single coating tracks results over AISI 4140 employing different laser power (a) 250W, (b) 350W, (c) 450W, and constant 300 mm/min travel speed.

[DOI: 10.22068/ijmse.3206]

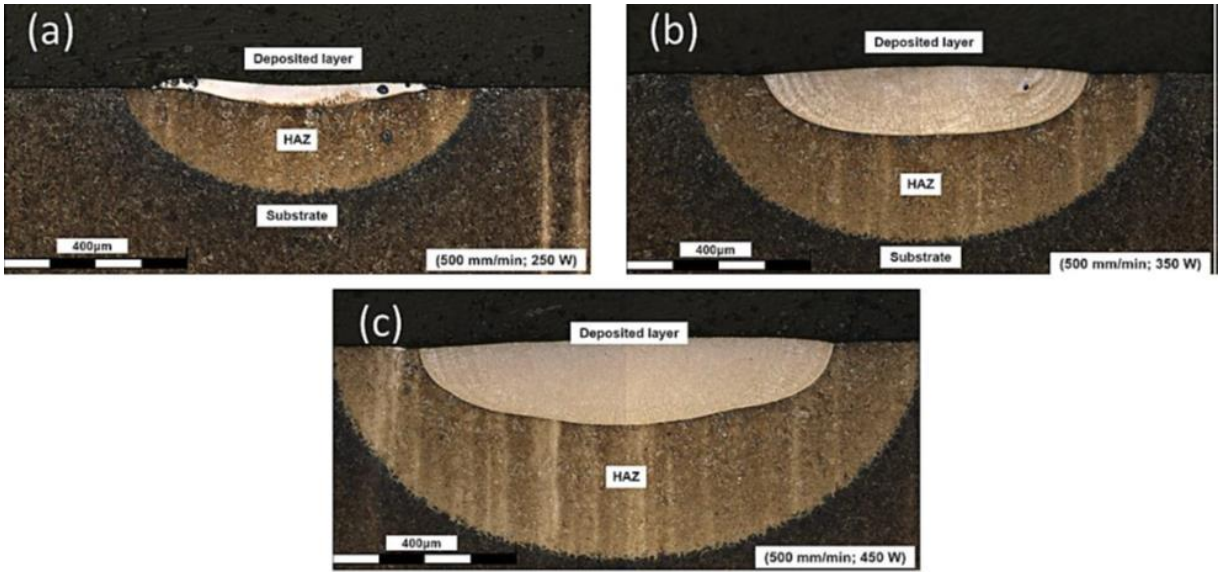

Fig. 5. Single coating tracks results over AISI 4140 employing different laser power (a) 250 W, (b) 350 W, (c) 450 W, and constant 500 mm/min travel speed.

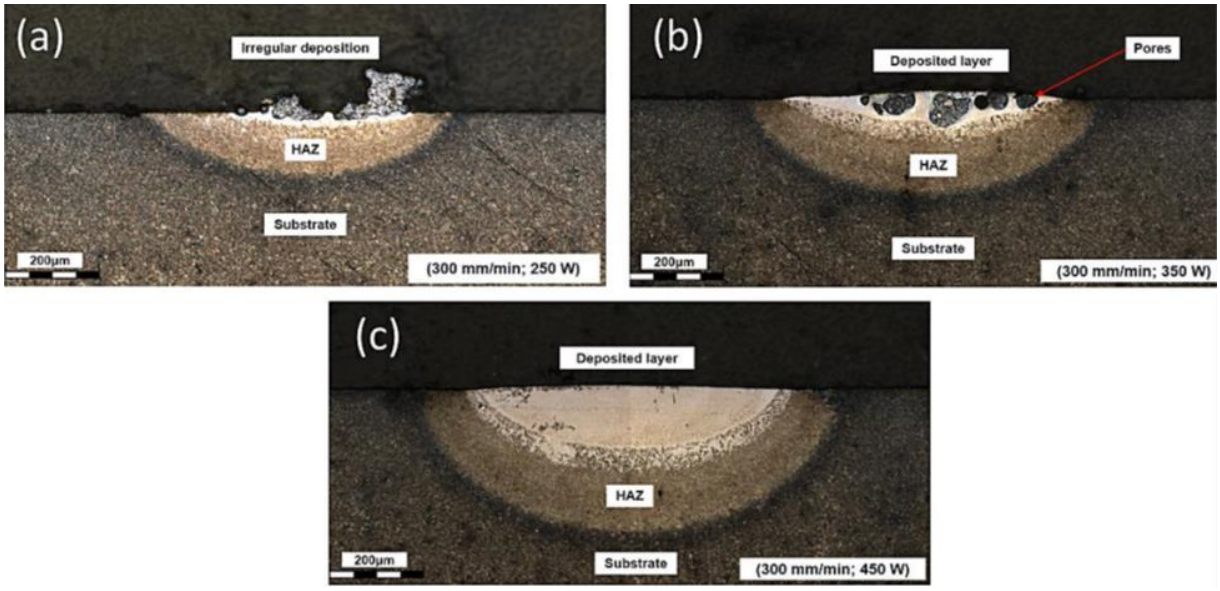

Fig. 6. Single coating tracks results over AISI H13 employing different laser power (a) 250 W, (b) 350 W, (c) 450 W, and constant 300 mm/min travel speed.

Among the other configurations, the one with the lowest HAZ and good deposition was the combination us-ing a deposition speed of 500 mm/min and a power of 250 W, thus defining the parameter for the deposition for both substrates.

Once the parameters were defined (500 mm/min; 250 W), a single layer was deposited in a sufficient region to carry out future tests. After the cladding process, it was possible to observe a thin and homogeneous depos-ited layer and the Heat Affected Zone (HAZ) of each path traversed by the laser. Very few pores and few cracks were also observed in some compositions, but they did not affect the final quality, without delamination. Figure 8 shows the cross-sections of the deposited layers using the defined parameters.

The laser cladding process allows for precise control over the thickness of the coating, making it possible to produce high-quality thin coatings with thicknesses as low as a few micrometers for this specific case the coating achieved a thickness less of 100 µm. Upon comparison of the images of the coated samples obtained during the present study with the results reported by [44] employing

[DOI: 10.22068/ijmse.3206]

the HVOF technique to deposit WC-CO coatings for the deposition of WC-CO coatings onto an AISI 1008 substrate, a notable decrease in the porosi-ty was observed. This finding is of significance, particularly concerning corrosion protection. To have a more detailed view of the substrate compared with the HAZ region, additional images were performed and present-ed in Figure 9 (a) is possible to see the heat affecting zone of the AISI 4140 substrate and in (b) the substrate without HAZ or cladding effects.

The optical analysis discloses a well-defined Heat-Affected Zone (HAZ) characterized by its limited extent. Subsequent to the cladding process, no substantial modifications in the fundamental properties of the sub-strate have been discerned. This outcome is fundamentally attributed to the process's inherently localized na-ture, facilitating precise material deposition onto discrete substrate areas without compromising its overall bulk properties. Consequently, coatings applied by the cladding process permit minimal thermal impact on the sub-strate. Figure 10 shows the HAZ region (a) and substrate for AISI H13 material.

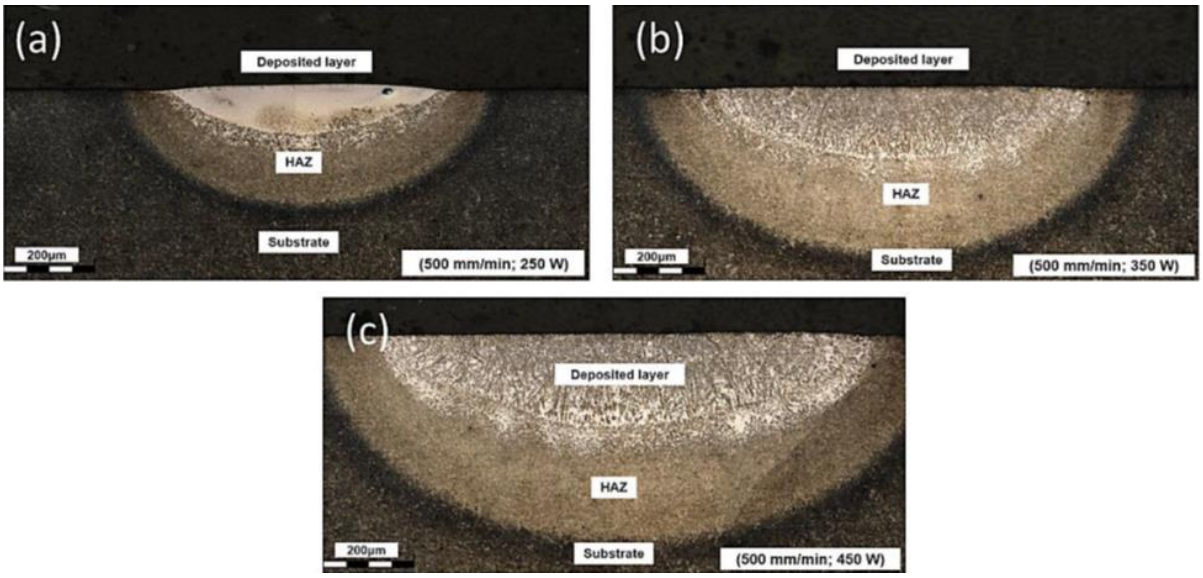

Fig. 7. Single coating tracks results over AISI H13 employing different laser power (a) 250 W, (b) 350 W, (c) 450 W and con-stant 500 mm/min travel speed.

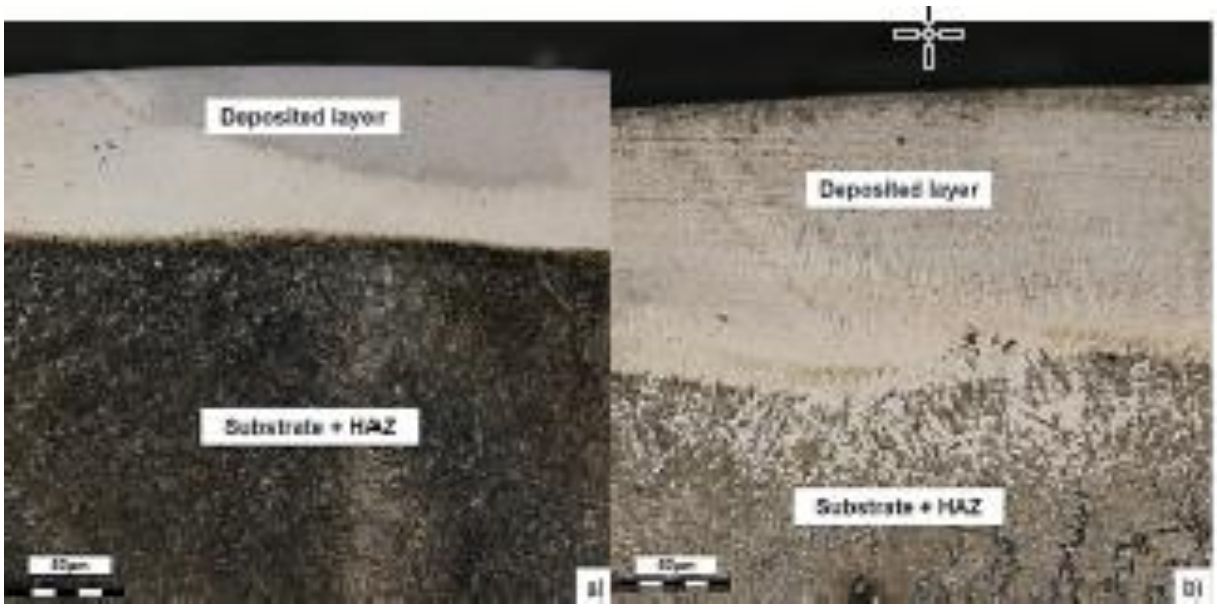

Fig. 8. Detail of WC-17Co deposited on AISI 4140 (a) and AISI H13 (b).

[DOI: 10.22068/ijmse.3206]

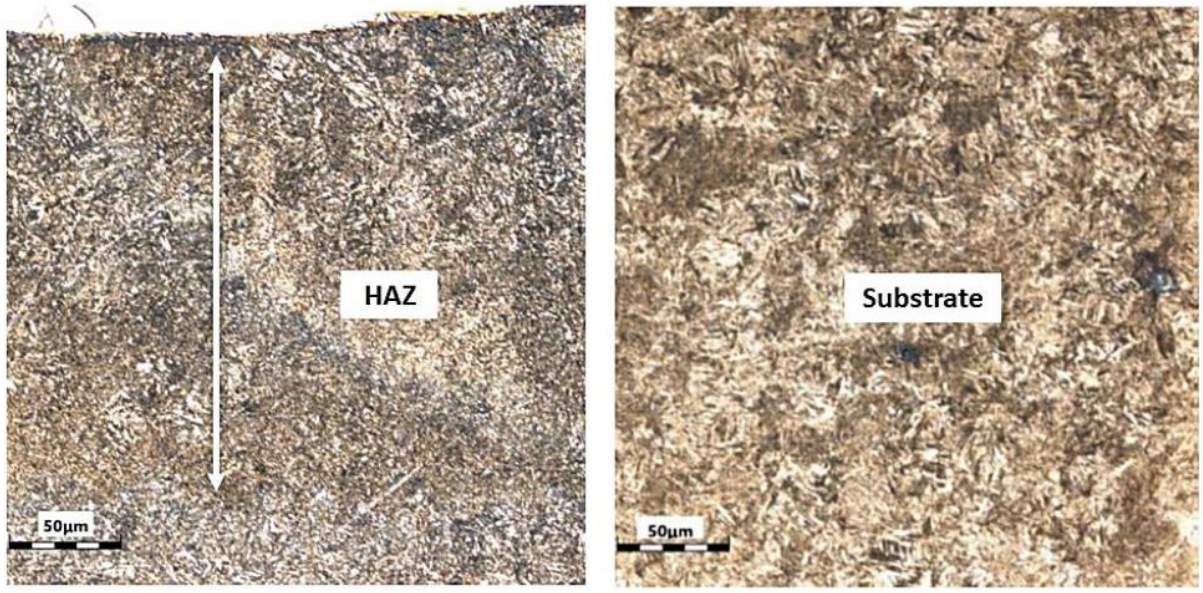

(a) …… (b)

Fig. 9. Detail of the HAZ (a) and substrate (b) AISI 4140.

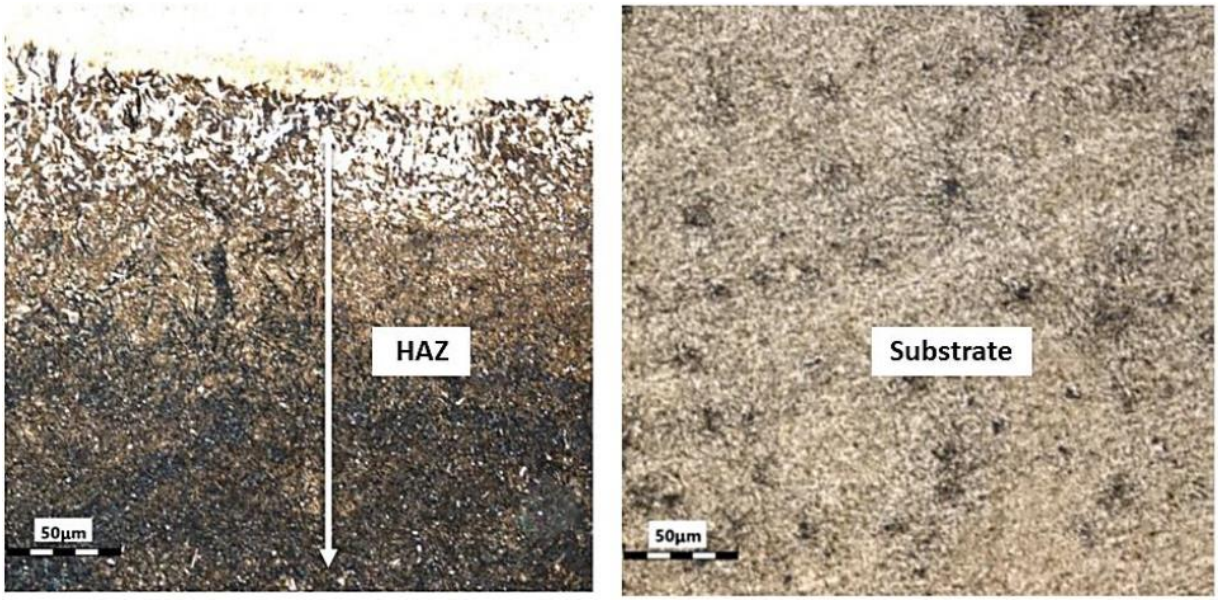

(a) (b)

Fig. 10. Detail of the HAZ (a) and substrate (b) AISI H13.

Table 2 provides a comprehensive overview of the average microhardness outcomes attained from the fab-ricated samples, facilitating a direct juxtaposition with the microhardness metrics inherent to the substrate. The outcomes conspicuously illustrate that both coating processes engendered augmented surface hardness. Additionally, it warrants attention that carried out deposition manifested substantial mechanical improvements, evidenced by an average microhardness value surpassing the substrates by 80%. It is salient to highlight that the derived values align comparably with those elucidated by [10], wherein a diverse range of deposition methodologies encompassing HVOF, warm spraying, and cold spraying (CS) were employed. It is of para-mount import to underscore that the significance of these findings rests upon their contextual dependency on the precise test conditions orchestrated and the intrinsic material properties harnessed in the experimental en-deavor.

[DOI: 10.22068/ijmse.3206]

Table 2. Average measurements of microhardness tests.

	Substrate	WC-17Co
AISI H13	578,42 ± 35,51 HV	935,35 ± 128,25 HV
AISI 4140	532,51 ± 34,31 HV	973,53 ± 137,38 HV

Vickers microhardness profiles were also made for each sample, starting from the surface towards the sub-strate. Figures 11 and 12 show the hardness gradient results as it moves away from the surface and the de-posited layer. It is also possible to identify the behavior of the Heat Affected Zone (HAZ).

The stratum immediately subsurface exhibits elevated levels of hardness, succeeded by a marked diminu-tion in hardness magnitudes that corresponds to the segment of the substrate manifesting altered properties ensuing from the processing regimen; specifically, the region designated as the Heat Affected Zone (HAZ). The fluctuations in hardness within the HAZ locality are presumed to stem from the rapid thermal oscillations induced by the laser's thermal input, engendering consequential thermal cycling. These thermal dynamics, precipitated by the laser, engender a perturbation in the dislocation mobility within the material, thereby exert-ing an influence on its hardness characteristics.

Immediately after the HAZ, a restitution of the microhardness values to a state approximating the character-istic metric of the substrate, hitherto gauged, becomes evident. Given the discrepant thicknesses across the specimen samples, the acquisition of data for the construction of the microhardness profile is terminated upon the normalization of said substrate values. It is noteworthy, however, that the variances in hardness do not appear to occasion any discernible alteration in the metallurgical interconnection originating from the laser cladding process between the applied coating and the substrate.

Illustrations denominated as Figures 13 and 14 delineate the micro-adhesive wear behaviors exhibited by the substrates, concomitantly juxtaposed with the findings emanating from the engendered layers.

The behavior exhibited by the coating material evinces noteworthy enhancements in terms of its wear re-sistance vis-à-vis the distinct base materials employed within the substrate. As discernible from the figures, discernable shifts in the trajectory of material removal become apparent as the wear test progresses, a phe-nomenon potentially ascribable to the accrual of plastic deformation and damage within the material matrix. Concurrently, the frictional forces generated during the test impart thermal energy due to the intimate interac-tion between the spherical probe and the material surface. The resultant elevated temperatures wield the ca-pacity to impart discernable influence upon the mechanical properties inherent to the material, consequently influencing its susceptibility to deformation and, by extension, augmenting the propensity for material removal.

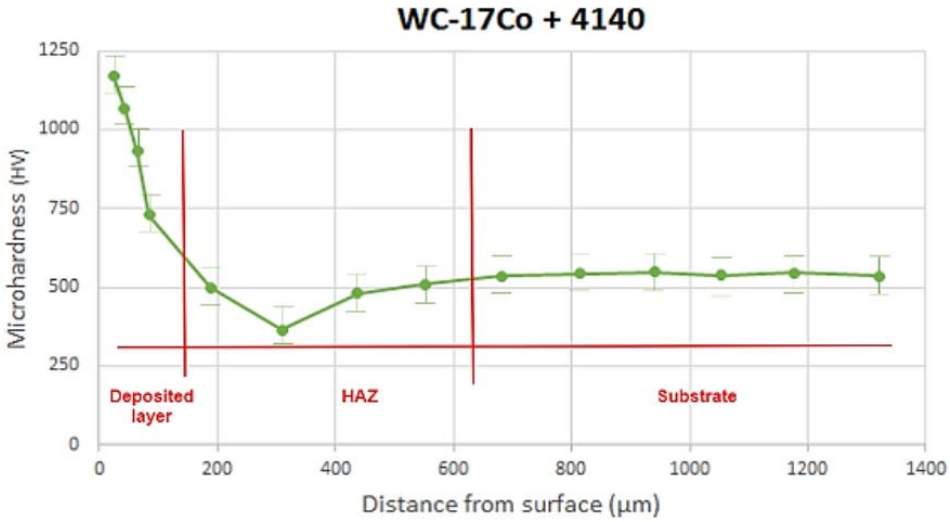

Fig. 11. Vickers microhardness WC-17Co/AISI 4140.

[DOI: 10.22068/ijmse.3206]

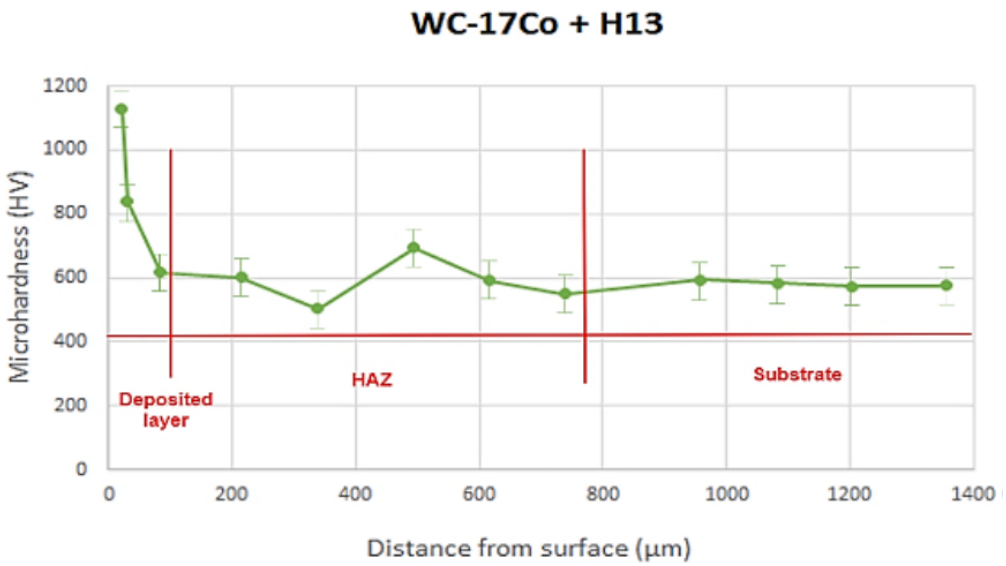

Fig. 12. Vickers microhardness WC-17Co/AISI H13.

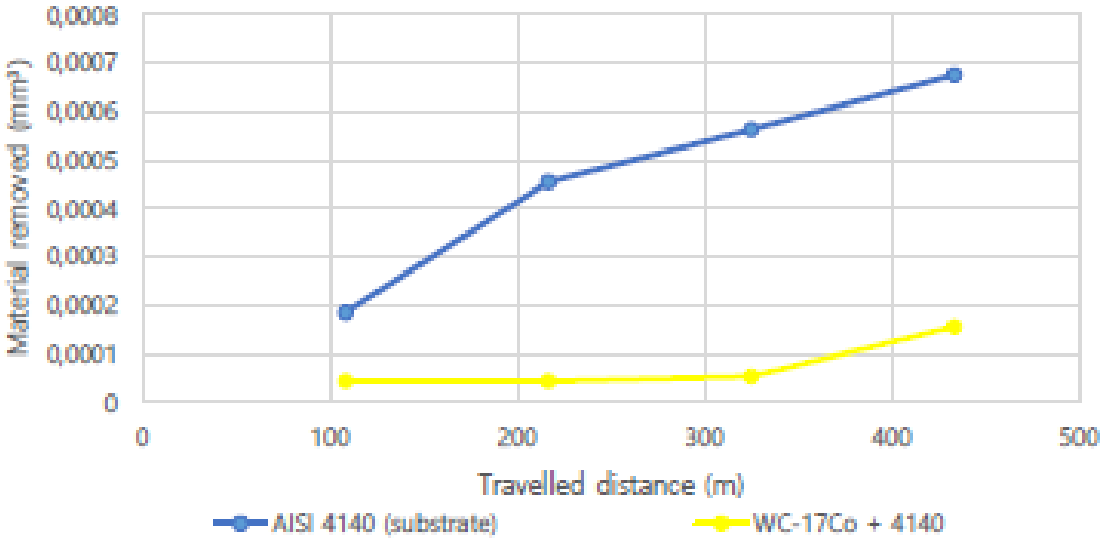

Fig. 13. Microadhesive wear tests WC-17Co/AISI 4140.

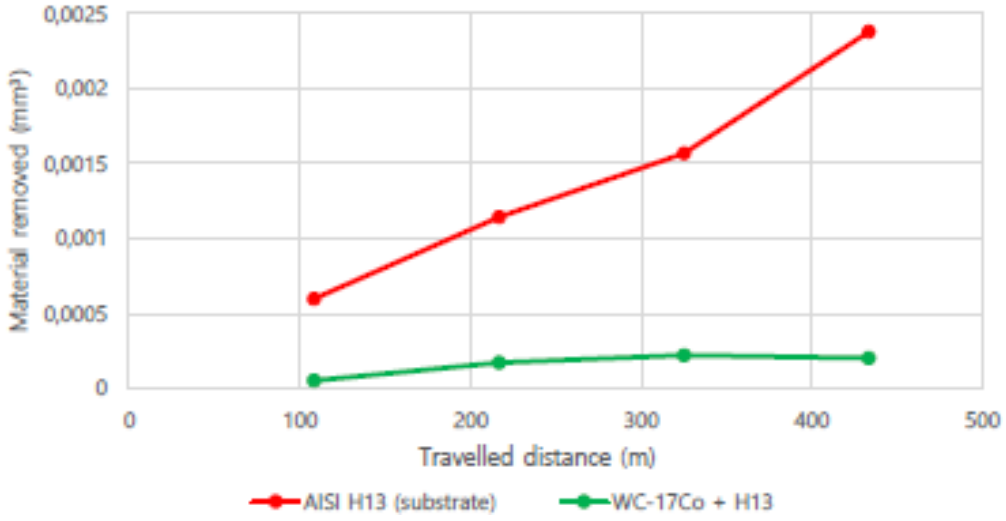

Fig. 14. Microadhesive wear tests WC-17Co/AISI H13.

[DOI: 10.22068/ijmse.3206]

The graph presented herein illustrates the intricate correlation between the distance traversed (measured in meters) and the corresponding volume of material removed (measured in cubic millimeters). This removal transpires as a direct outcome of the rotational motion exhibited by the sphere subjected to testing. The re-sultant coatings evince a marked augmentation in wear resistance when juxtaposed with their corresponding substrates, thereby notably amplifying the overall wear-resistant attributes of the substrate material.

Upon an exhaustive examination of the volume removal outcomes gleaned from the fabricated specimens, it becomes evident that a striking congruence is discernible in the deposition values of WC-17Co across both substrates under investigation. In succinct recapitulation, the laser cladding procedure engenders thin coatings of exceptional caliber, characterized by minimal porosity and a heightened degree of adhesion to the substrate. These attributes collectively culminate in the outperformance of the heretofore documented results ascribed to High-Velocity Oxygen Fuel (HVOF) or Cold Spray methodologies [10, 44–46].

Crucially, it is imperative to accentuate that the nuances within the observed behaviors are innately reliant upon the intrinsic material characteristics subjected to scrutiny, the amplitude of the applied load, and the specific ambient conditions prevailing during the execution of the testing protocol.

4. DISCUSSION

The results show that different laser power levels (250 W, 350 W, and 450 W) had a significant impact on the quality of the coatings. When using the lowest laser power of 250 W, a non-deposition condition was observed, indicating that the energy input was insufficient to create a stable coating. At 350 W, irregular deposition was observed, and at 450 W, a porous coating resulted. These observations suggest that precise control of laser power is crucial for achieving desired coating properties. The study also examined the effect of travel speed on the coating quality. A travel speed of 500 mm/min consistently produced good WC-17Co coatings on both substrate materials. However, at the highest laser power (450 W) and the same travel speed, a large Heat Af-fected Zone (HAZ) was observed, which might be undesirable for certain applications. This finding highlights the importance of optimizing both laser power and travel speed for specific coating requirements.

The microhardness measurements revealed that the coatings significantly increased the surface hardness of the substrates. The coatings exhibited an average microhardness value surpassing that of the substrates by 80%, indicating improved mechanical properties. For its part wear tests demonstrated that the WC-17Co coat-ings exhibited superior wear resistance compared to the base materials. As the wear test progressed, noticea-ble shifts in material removal were observed, likely due to plastic deformation and thermal effects generated during the test. The coatings displayed an enhancement in hardness and wear resistance that is essential for applications requiring increased material durability.

When compared the laser cladding process results with those obtained using other deposition techniques, such as High-Velocity Oxygen Fuel (HVOF) or Cold Spray. It was found that the laser cladding process re-sulted in coatings with minimal porosity and high adhesion to the substrate. These attributes make laser clad-ding a promising method for achieving high-quality coatings, especially in applications where corrosion protec-tion and wear resistance are critical.

The presented results demonstrate the effectiveness of laser cladding for depositing WC-17Co coatings on different substrates. The choice of laser power and travel speed is crucial for achieving the desired coating properties, including minimizing the HAZ and optimizing microhardness and wear resistance. Laser cladding offers a viable alternative to traditional deposition methods, with the potential to produce thin, high-quality coatings suitable for various engineering applications. However, it's important to note that the success of laser cladding depends on factors like material characteristics, applied load, and ambient conditions, which should be considered when applying this technique in real-world scenarios.

5. CONCLUSIONS

For the composition studied, it was established

[DOI: 10.22068/ijmse.3206]

that configurations using the combination of a deposition ve-locity of 500 mm/min and a power of 250 W produce the best quality layers, with little or no presence of pores and cracks or detachment of the deposited material. Also, it results in a smaller HAZ, an important factor to be analyzed, since, in a layer-by-layer construction process, a very large HAZ can affect microstructures and properties of already deposited layers and consequently present geometric distortions and/or residual stresses.

When using tool steel (AISI H13) as substrate, the deposition intends to increase the interesting properties for applications of these materials, such as hardness and wear resistance, both very important for molds and tooling where these properties are highly demanded. Also, when using alloyed steel (AISI 4140), widely used for the manufacture of mechanical components due to its medium mechanical strength and fracture resistance, it still needs properties such as wear resistance to amplify its applications. As a result, the deposition of both compositions in the parameter defined as ideal, resulted in an increase in hardness and wear resistance, which demonstrates the fulfillment of the objective of the work. In this way, from the characterized coatings and the optimized process in the study, it is possible to solve very common problems of deterioration by tribological processes, providing different improved mechanical properties and improving their performance and the tool life.

The use of the selected cladding material is a highly effective way to improve the wear resistance of the samples, but careful consideration of the composition and processing parameters is essential to achieve the desired properties. The wear resistance offered by the cladding material is a function of the high densities of hard, wear-resistant WC particles enclosed in a soft, ductile metallic Co binder giving WC-Co cemented car-bides their wear resistance and toughness.

The minimal changes observed in the substrate properties make the laser cladding process an attractive op-tion for coating applications, particularly in cases where the substrate material is critical to the overall perfor-mance of the component or system. By preserving the original properties of the substrate, laser cladding pro-vides a reliable and efficient means of enhancing the surface properties of the substrate, without compromis-ing its overall integrity or functionality.

Notwithstanding the outcomes derived from this study, it remains crucial for forthcoming endeavors to ap-praise fluctuations within operational parameters. Notably, the amplification in temperature encountered by components fabricated from H13 steel over the course of their service life warrants meticulous investigation. This course of action is essential for obtaining a more nuanced understanding of the coating's efficacy under such circumstances.

ACKNOWLEDGMENTS

Authors acknowledge the financial support of the São Paulo Research Foundation (FAPESP)– grant num-bers: 2016/11309-0 and 2019/26362-2. National Council for Scientific and Technological Development (CNPq) process n. 305294/2015-6. C.

REFERENCES

[1]. Ghadami, F., Sohi, H., and Ghadami, S., “Effect of TIG surface melting on the structure and wear properties of air plasma-sprayed WC– Co coatings,” Surf. Coat. Technol., 2015, 261, 108–113.

[2]. Ding, X., Ke, D., Yuan, C., Ding, Z., and Cheng, X., “Microstructure and Cavitation Erosion Resistance of HVOF Deposited WC-Co Coatings with Different,” Coatings, 2018, 8, 307.

[3]. Liu, J., Chen, T., Yuan, C., and Bai, X., “Effect of corrosion on cavitation erosion behavior of HVOF sprayed cobalt-based coatings,” Mater. Res. Express, 2022, 9, 066402.

[4]. Mirhosseini, S., and Mahboubi, F., “Effect of plasma nitriding on tribological properties of nickel‑boron-nanodiamond electroless coatings,” Surf. Coat. Technol., 2022, 435, 128216.

[5]. Wang, L., Li, L., and Kuang, X,. “Effect of substrate bias on microstructure and mechanical properties of WC- DLC coatings deposited by HiPIMS,” Surf. Coat. Technol., 2018, 352, 33–41.

[6]. Aghajani, H., Hadavand, E., Peighambardoust, N., and Khameneh-asl, S., “Electro spark deposition of WC– TiC– Co– Ni cermet coatings on St52 steel,”

[DOI: 10.22068/ijmse.3206]

Surfaces and Interfaces, 2020, 18, 100392.
[7]. Silva, F., et al., "Corrosion behavior of WC-Co coatings deposited by cold gas spray onto AA," Corros. Sci., 2018, 136, 231–243.
[8]. Zhang, J., Lei, J., Gu, Z., Tantai, F., Tian, H., and Han, J., "Effect of WC-12Co content on wear and electrochemical corrosion properties of Ni-Cu/WC-12Co composite coatings deposited by laser cladding," Surf. Coat. Technol., 2020, 393, 125807.
[9]. Jiao, x., Wang, J., Wang, C., Gong, Z., Pang, X., and Xiong, S., "Effect of laser scanning speed on microstructure and wear properties of T15M cladding coating fabricated by laser cladding technology," Opt. Lasers Eng., 2017, 110,163–171.
[10]. Chen, X., Li, C., Gao, Q., Duan, X., and Liu, H., "Comparison of Microstructure, Microhardness, Fracture Toughness, and Abrasive Wear of WC-17Co Coatings Formed in Various Spraying Ways," Coatings, 2022, 12, 814.
[11]. Kudryashov, A., Lebedev, D., Potanin, A., and Levashov, E., "Structure and properties of coatings produced by pulsed electro spark deposition on nickel alloy using Mo-Si-B electrodes," Surf. Coat. Technol., 2017, 335, 104–117.
[12]. Korkmaz, K., "Investigation and characterization of electrospark deposited chromium carbide-based coating on the steel," Surf. Coat. Technol., 2015, 272, 1–7.
[13]. Aw P., and Tan, B., "Study of microstructure, phase and microhardness distribution of HVOF sprayed multi-modal structured and conventional WC–17Co coatings," J. Mater. Proc. Tech. 2006, 305–311.
[14]. Fayyazi, S. "Optimizing High-Velocity Oxygen Fuel-Sprayed WC – 17Co Coating Using Taguchi Experimental Design to Improve Tribological Properties," Trans. Indian Inst. Met., 2018, 71, 3045–3062.
[15]. Joshi, S., "Effect of spray angle and substrate material on formation mechanisms and properties of HVAF sprayed coatings," Surface and Coating Technology, 2022, 452,129115.
[16]. Barragan, G., Ferreira, R., Edson, F., and Eraldo, M., "Study of the surface roughness of a remanufactured bimetallic AISI 1045 and 316L SS part obtained by hybrid manufacturing (DED/HSM)," Int. J. Adv. Manuf. Technol., 2023, 124, 3185-3199.
[17]. Roberto C., et al., "Study of the Wear and Corrosion Performance of Hard Coatings Applied by Different Processes on Low Carbon Steel," Materials Sciences and Applications, 2016, 7, 358-370.
[18]. Hajiannia, I., Shamanian, M., Atapour, M., Ashiri, R., and Ghassemali, E., "Synthesis of Fe-TiC Hard Coating From Ilmenite Via Laser Cladding," Iran. J. Mater. Sci. Eng., 2019, 16, 79–88.
[19]. Li, N., Huang, S., Zhang, G., Qin, R., Liu, W., and Xiong, H., "Progress in additive manufacturing on new materials : A review," J. Mater. Sci. Technol., 2019, 35, 242–269.
[20]. Debroy, T., et al., "Additive manufacturing of metallic components– Process, structure and properties," Progress in Materials Science, 2018, 92, 112–224.
[21]. Barragan, G., Rojas, D., Grass, J., and Coelho, R., "Observations on Laser Additive Manufacturing (LAM) in Terms of Directed Energy Deposition (DED) with Metal Powder Feedstock," Lasers Eng., 2021, 50, 117–141.
[22]. B. Graf, "3D laser metal deposition : process steps for additive manufacturing," Welding in the world, 2018, 62, 877–883.
[23]. Wang, T., Zhu, L., Song, H., and Wang, H., "Effect of WC-17Co content on microstructure and properties of IN718 composites prepared by laser cladding," Opt. Laser Technol., 2021, 148, 107780.
[24]. Stewart, D., Shipway, P., and McCartney, D., "Abrasive wear behaviour of conventional and nanocomposite HVOF-sprayed WC-Co coatings," Wear, 1999, 225–229, 789–798.
[25]. Ang, A., Berndt, C., and Cheang, P., "Deposition effects of WC particle size on cold sprayed WC-Co coatings," Surf. Coatings Technol., 2011, 205, 3260–3267.
[26]. Wood, R., "Tribology of thermal sprayed WC-Co coatings," Int. J. Refract. Met. Hard Mater., 2010, 28, 82–94.
[27]. Matthews, S., Ansbro, J., Berndt, C., and

[DOI: 10.22068/ijmse.3206]

Ang, A., "Carbide dissolution in WC-17Co thermal spray coatings: Part 1-project concept and as-sprayed coatings," J. Alloys Compd., 2021, 856, 157464.
[28]. Erfanmanesh, M., Abdollah-pour, H., and Mohammadian-Semnani, H., "An empirical-statistical model for laser cladding of WC-12Co powder on AISI 321 stainless steel," Opt. Laser Technol., 2017, 97, 180–186.
[29]. Manoj, M., Burela, R., Dzhurinskiy, D., Babu, A,. Gupta, A., and Harursampath, D., "Thermo-Mechanical Finite Element Analysis of the Laser Heat Treatment of WC-17Co Thermally Sprayed Coating," Proceedings of the International Thermal Spray Conference, Vienna, Austria, 2022, 928–938.
[30]. Sun, G., Song, L., and Mazumder, J., "Microstructure and Wear Behavior of Laser-Aided Direct Metal Deposited Co-Microstructure and Wear Behavior of Laser-Aided Direct Metal Deposited Co-285 and Co-285 + WC Coatings," Metallurgical and Materials Transactions A, 2010, 41, 1592-1603.
[31]. Zhang, G., et al., "Effect of laser beam incidence angle on cladding morphology in laser cladding process," J. Mech. Sci. Technol., 2020, 34, 1531–1537.
[32]. Sun, W., Zhang, D., Chen, X., Wang, K., Zhang, J., and Jia, Y., "Effect of the scanning speed of laser cladding on microstructure and mechanical properties of WC/Ni composite coatings," J. Mech. Sci. Technol., 2022, 36, 679–687.
[33]. Erfanmanesh, M., Abdollah-Pour, H., Mohammadian-Semnani, H., and Shoja-Razavi, R., "Kinetics and oxidation behavior of laser clad WC-Co and Ni/WC-Co coatings," Ceram. Int., 2018, 44, 12805–12814.
[34]. You, A., et al., "Effect of linear energy density on microstructure and wear resistance of WC-Co-Cr composite coating by laser cladding," Surf. Coatings Technol., 2022, 454, 129185.
[35]. Erfanmanesh, M., Shoja-Razavi, R., Abdollah-Pour, H., Mohammadian-Semnani, H., Barekat, M., and Hashemi, S., "Friction and wear behavior of laser cladded WC-Co and Ni/WC-Co deposits at high temperature," Int. J. Refract. Met. Hard Mater., 2018, 81, 137–148.
[36]. Yuan, J., Ma, C., Yang, S., Yu, Z., and Li, H., "Improving the wear resistance of HVOF sprayed WC-Co coatings by adding submicron-sized WC particles at the splats' interfaces," Surf. Coatings Technol., 2016, 285, 17–23.
[37]. BeAM Machines, "Modulo 250 Technical Documentation." BeAM, 2022. https://www.beam-machines.com/products/modulo250.
[38]. Barragan, G., Mariani, F., and Coelho, R., "Application of 316L stainless steel coating by Directed Energy Deposition process Application of 316L stainless steel coating by Directed Energy Deposition process," IOP Conference Series: Materials Science and Engineering, 2021, 1154, 012014.
[39]. ASTM, "Standard Test Method for Microindentation Hardness of Materials 1," 2017.
[40]. Cozza, R., de Mello, J., Tanaka, D., and Souza, R., "Relationship between test severity and wear mode transition in micro-abrasive wear tests," Wear, 2007, 263, 1-6 SPEC, 111–116.
[41]. Rutherford, K., and Hutchings, I., "A micro-abrasive wear test, with particular application to coated systems," Surf. Coatings Technol., 1996, 79, 231–239.
[42]. Gant, A., and Gee, G., "A review of micro-scale abrasion testing," J. Phys. D. Appl. Phys., 2011, 44, 073001.
[43]. Esteves, P., de Macêdo, M., Souza, R., and Scandian, C., "Effect of ball rotation speed on wear coefficient and particle behavior in micro-abrasive wear tests," Wear, 2019, 426–427, 137–141.
[44]. Lamana, M., Pukasiewicz, A., and Sampath, S., "Influence of cobalt content and HVOF deposition process on the cavitation erosion resistance of WC-Co coatings," Wear, 2018, 398–399, 209–219.
[45]. Tillmann, W., et al., "Microstructural characteristics of high-feed milled HVOF sprayed WC-Co coatings," Surf. Coatings Technol., 2019, 374, 448–459.
[46]. Qiao, L., Wu, Y., Hong, S., Long, W., and Cheng, J., "Wet abrasive wear behavior of WC-based cermet coatings prepared by

[DOI: 10.22068/ijmse.3206]

HVOF spraying," Ceram. Int., 2021, 47, 1829–1836.

[DOI: 10.22068/ijmse.3206]